Control Architectures for Metamaterials in Vibration Control

Buskes, V. F.; Kaczmarek, M. B.; Veenstra, J. C.; Coulais, C.; Hosseinnia, S. H.

DOI
10.1109/ICM54990.2023.10101931

Publication date
2023

Document Version
Final published version

Published in
Proceedings - 2023 IEEE International Conference on Mechatronics, ICM 2023

Control Architectures for Metamaterials in Vibration Control

V.F. Buskes*, M.B. Kaczmarek*‡, J.C. Veenstra†, C. Coulais† and S.H. HosseinNia*
*Department of Precision and Microsystems Engineering, Delft University of Technology, Delft, The Netherlands
†Institute of Physics, University of Amsterdam, Amsterdam, The Netherlands
Email: ‡m.b.kaczmarek@tudelft.nl

2023 IEEE International Conference on Mechatronics (ICM) | 978-1-6654-6661-5/23/$31.00 ©2023 IEEE | DOI: 10.1109/ICM54990.2023.10101931

***Abstract*—Metamaterials are artificial structures with properties that are rare or non-existent in nature. These properties are created by the geometry and interconnection of the metamaterial unit cells. In active metamaterials, sensors and actuators are embedded in each unit cell to achieve greater design freedom and tunability of properties after the fabrication. While active metamaterials have been used in vibration control applications, the influence of applied control architectures on damping performance has not been thoroughly studied yet. This paper discusses the relationship between suitable control architectures for increased damping in finite active metamaterials and the number of damped modes. A metamaterial beam consisting of links with measured and actuated joints is considered. Optimal controllers for each of the considered scenarios are designed in the modal domain using linear-quadratic regulator (LQR). We show that, when all modes of a structure should be damped, the optimal solution can be reduced to a decentralised controller. When modes in a smaller range of frequencies are targeted, distributed controllers show better performance. The results are confirmed with experiments.**

***Index Terms*—Mechatronic Systems, Vibration Control, Metamaterials, Active metamaterials, Decentralised control**

I. Introduction

Metamaterials are artificial materials that exhibit properties not commonly found in nature. For example, electromagnetic metamaterials can achieve negative permeability and permittivity [1]. Optical metamaterials are used for their negative refractive index to bend light in the opposite direction [2]. Mechanical metamaterials can have a negative Poisson ratio or negative Young's modulus [3]. These exotic properties are a result of the periodic arrangement of specifically tailored unit cells to form large lattice structures.

Among those properties, the ability to strongly attenuate vibrations has sparked great interest in vibration isolation and damping applications [4]. The metamaterials can be used not only to attenuate resonances in finite structures but also to prevent the transmission of vibrations in certain frequency ranges. Such band gaps can originate from the Bragg scattering effect or from the inclusion of resonators in unit cells.

By including sensors, actuators and controllers within the lattice structure, new qualities can be obtained that were previously limited by the passiveness of the material [5]–[7]. Active elements allow for virtual material properties like real-time stiffness and damping control without requiring additional mass or damping elements. For example, in [8] a metamaterial can alter its elastic modulus based on the internal displacement of the unit cell. In [9] piezoelectric material is used to increase the active damping component of a flexible metamaterial beam.

While active metamaterials have gained increased attention throughout the last few years, studies on suitable control architectures for these materials are still limited. In fact, literature on active metamaterials is predominantly based on decentralised control alone [9]–[11]. This means that every sensor and actuator pair is controlled by a local Single-Input Single-Output (SISO) controller. The reason for this is often based on practicality. First of all, the controller complexity is independent on the amount of unit cells, which makes it applicable for large systems. Secondly, the wiring and integration of such controllers are straightforward when implemented on a practical system. Lastly, it allows for the design of the material on a unit cell level instead of on a global scale. However, whether decentralised control results in optimal performance is unclear.

On the other hand, centralised control, in which all unit cells are connected to a single master control unit, may yield better results. This is possible because all available information is combined and utilised for control, which can be achieved with optimal Multi-Input Multi-Output (MIMO) control techniques like linear-quadratic regulator (LQR) or H_∞ control. Another example of a centralised control approach is modal control. However, implementing a centralised solution is challenging for large systems due to the fact that extensive amounts of wiring are necessary, let alone the computational power that is required [12].

Between these two extrema, a distributed control architecture is a middle-ground solution for metamaterials. In this case, decentralised controllers are used that can also communicate with neighbouring sensors. This architecture offers greater design freedom than in the decentralised case and remains scalable for implementation in large-scale metamaterials. In [13] and [14], distributed control has been shown effective for systems sharing some properties of metamaterials, like infinite-sized interconnected mass-spring systems and vehicle platoons. This was done by showing that the optimal LQR feedback matrix in the Spatial Fourier Domain is inherently localised. However, in these papers systems with absolute measurements were considered, whereas active metamaterials are limited to relative measurements.

This paper investigates the effect of the control architecture on the damping performance of metamaterial structures with relative measurements. More specifically, we design optimal LQR controllers in the modal domain to damp specific modes of the system and determine if any localisation is present in the feedback matrix. To the best of our knowledge, this has not been researched yet for metamaterials. We consider a finite metamaterial beam with six discrete elements forming a 1D grid of unit cells. Each element consists of a joint with active sensing and actuation capabilities.

The paper is structured as follows. In Section II, the model is given for the metamaterial beam. In Section III, theory on LQR is given, which is used to demonstrate the optimal control structure for this beam in modal domain. In Section IV, experiments are performed to validate the numerical simulations. The paper ends with a conclusion in Section V.

II. Model

In this section, the model for the finite metamaterial beam is set up, which is based on the schematic in Fig. 1. Rigid beams of length l and flexible "smart" joints alternate to form a discretized flexible structure. The joints can measure the relative angular displacement θ_n and apply a control torque τ_n. They each have a mass m and rotational stiffness k.

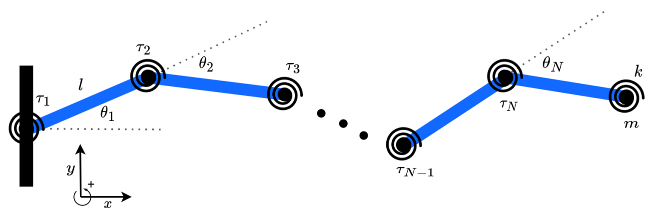

Fig. 1: Metamaterial beam with relative coordinates and torque-actuated joints.

A linear algebraic model is constructed by deriving the mass and stiffness matrices of the system

$$M = \frac{\partial^2 T}{\partial\dot{\theta}\partial\dot{\theta}}, \qquad K = \frac{\partial^2 V}{\partial\theta\partial\theta}. \tag{1}$$

Here T is the kinetic energy, V the potential energy and $\theta = \begin{bmatrix}\theta_1, \dots, \theta_N\end{bmatrix}$ represents the angular displacements of each joint. The potential energy is directly computed as

$$V = \frac{1}{2} k \sum_1^N \theta_n^2. \tag{2}$$

The kinetic energy is computed by first defining the displacements $p = \begin{bmatrix}p_2, \dots, p_{N+1}\end{bmatrix}^T$ of each joint in terms of relative angles

$$\begin{bmatrix} p_{n,x} \\ p_{n,y} \end{bmatrix} = \begin{bmatrix} p_{n-1,x} \\ p_{n-1,y} \end{bmatrix} + l \begin{bmatrix} \cos(\sum_1^n \theta_n) \\ \sin(\sum_1^n \theta_n) \end{bmatrix}, \tag{3}$$

where $p_1 = [0, 0]^T$. Then the Jacobian of the displacement vector is computed and multiplied with the derivatives of the rotations to obtain velocities of each mass

$$v = \nabla p \cdot \dot{\theta}. \tag{4}$$

Lastly, the kinetic energy is computed

$$T = \frac{1}{2} m v^T v. \tag{5}$$

The system is linearized around the zero equilibrium and the values of l, m and k can be taken as arbitrary. For this paper, N is taken as 6, which is relatively small but allows for the intuitive analysis of the results.

Through a modal transformation it is possible to obtain modal mass and stiffness matrices

$$\tilde{M} = \Phi^T M \Phi \qquad \tilde{K} = \Phi^T K \Phi, \tag{6}$$

where $\Phi^T \in \mathbb{R}^{6\times 6}$ contains the eigenmodes obtained through the eigenvalue problem $\det(K - \omega^2 M) = 0$. The modal mass and stiffness matrices are used in a state space model

$$\dot{x} = \underbrace{\begin{bmatrix} 0 & I \\ -\tilde{M}^{-1}\tilde{K} & 0 \end{bmatrix}}_{A} x + \underbrace{\begin{bmatrix} 0 \\ \tilde{M}^{-1}\Phi^T \end{bmatrix}}_{B} u \tag{7}$$

$$y = \begin{bmatrix} \Phi & 0 \\ 0 & \Phi \end{bmatrix} x$$

where the states $x \in \mathbb{R}^{12}$ represent modal angular displacements and velocities of each joint. The control vector $u = \begin{bmatrix}\tau_1, \dots, \tau_N\end{bmatrix}^T$ contains the active torques on each joint, $I \in \mathbb{R}^{6\times 6}$ is the identity matrix and $0 \in \mathbb{R}^{6\times 6}$ is a null matrix.

III. Control Architectures

In this section LQR is used on the beam model and the structure of the feedback matrix is analysed.

A. Linear-quadratic regulator

LQR is an optimal control method that minimises the quadratic objective function

$$\begin{aligned} J = &\int_0^\infty (x^T Q x + u^T R u)\mathrm{d}t \\ \text{s.t.} \quad & \dot{x} = Ax + Bu \end{aligned} \tag{8}$$

for a linear system [15]. The Q and R matrices are used to tune the response of the closed-loop system. Here $R \in \mathbb{R}^{6\times 6}$ is chosen as a constant diagonal matrix to penalise all control inputs equally. The diagonal entries in $Q \in \mathbb{R}^{12\times 12}$ are varied to damp specific modes, for example, $Q(N+1, N+1) = 1$ will only damp the first mode if all other entries are zero. The objective function is minimised by solving the Algebraic-Riccati-Equation (ARE), which results in an optimal centralised feedback matrix K with feedback control

$$u = -Kx. \tag{9}$$

Since a modal model is considered in this paper, this matrix needs to be reverted back to physical domain to obtain physical meaning from the states

$$K_{\text{physical}} = K\Phi^T, \tag{10}$$

where $K_{\text{physical}} = \begin{bmatrix} K_p & K_v \end{bmatrix}$ contains a stiffening part K_p and damping part K_v. By focusing on active damping elements only, K_p remains zero and can be neglected in the remaining analysis.

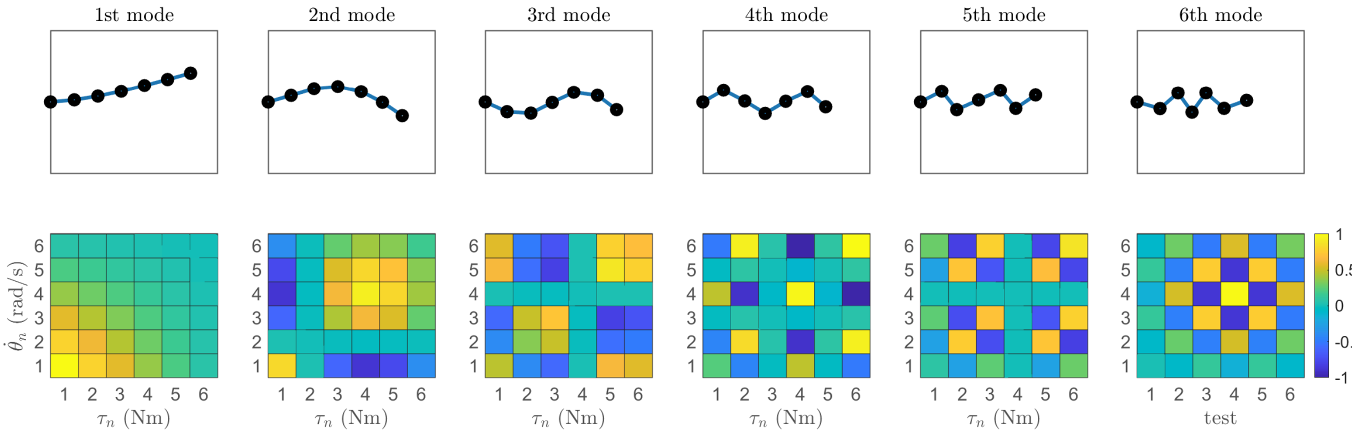

Fig. 2: For each mode of the beam (top) a LQR feedback matrix is computed (bottom). The matrix is plotted from a top-down view where the magnitude of each entry is indicated with a colour gradient on a range of -1 to 1. Only the velocity states are shown.

B. Analysis in modal domain

LQR is used with the A and B matrices from the state space model in (7). Since this model is in modal domain, it is possible to compute the optimal damping matrix for each individual mode of the beam, see Fig. 2. The result is obtained by using $Q = \begin{pmatrix} 0 & 0 \\ 0 & Q_v \end{pmatrix}$, where Q_v is a diagonal matrix whose non-zero term denotes the mode to be damped.

The matrices are displayed from a top-down view where each entry has been given a colour label based on its magnitude. Furthermore, the matrices show how each active torque τ_n is a function of multiple angular velocities θ_n to damp a specific mode. It can be seen that all damping matrices are full, i.e. almost all entries have gains. As a result, damping one specific mode would require a centralised controller, as each actuator requires information from all other sensors in the system. This control problem is closely related to modal control.

By damping multiple modes simultaneously, the structure of the LQR matrix changes. It will resemble a summation of several of the feedback matrices from Fig. 2. However, as many entries have either a positive or negative gain depending on which mode is damped, it is evident that combining these matrices will result in many entries adding up to zero. For example, in the extreme case where all modes are damped, it can be concluded that only the diagonal terms will remain non-zero as those are the only entries that have a common sign for all modes. A way of proving this is by applying the LQR algorithm to the beam with $Q = \begin{pmatrix} 0 & 0 \\ 0 & I \end{pmatrix}$, which damps all modes equally. The result of this is given in Fig. 3. As only the diagonal gains remain, the centralised solution can be reduced to six local decentralised controllers and it can be concluded that the optimal solution for damping all modes is by using a decentralised architecture.

In many applications, however, the desire is not to damp the whole frequency range, but focus on lower order modes as these have a larger contribution on the dynamics. It can

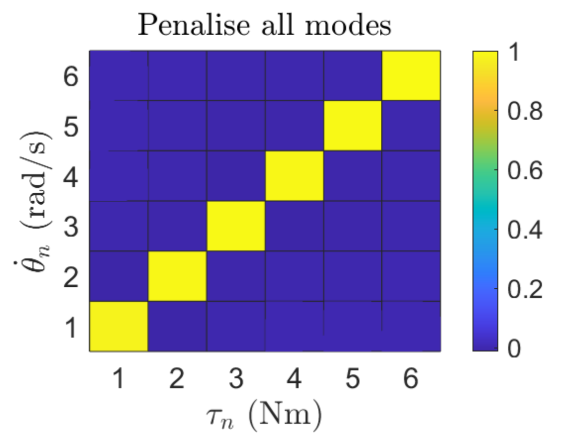

Fig. 3: The LQR feedback matrix if the whole frequency range is damped. Since the only gains in the matrix are on the diagonal, the optimal centralised matrix can instead be implemented by 6 independent decentralised controllers.

be shown that by excluding the fifth and sixth mode in the penalisation process, entries on the first upper and lower diagonals will also become non-zero. This is because the fifth and sixth mode are the only modes that have negative gains for all these entries, whereas all other modes have mostly non-negative entries there. In Fig. 4 the LQR algorithm is applied with additional penalisation of the first four modes by using $Q = \begin{pmatrix} 0 & 0 \\ 0 & Q_v \end{pmatrix}$, where $Q_v = \text{diag}(5, 5, 5, 3, 1, 1)$. It can be seen that the optimal control architecture is no longer decentralised, but also includes relatively high gains on the first upper and lower diagonal. In other words, damping lower order modes is more effective when information of the first neighbour sensors is included in each controller in addition to the local measurement that was already used. This is because those sensors mostly have the same rotational direction as the local measurement for lower order mode shapes. This control structure resembles a distributed architecture.

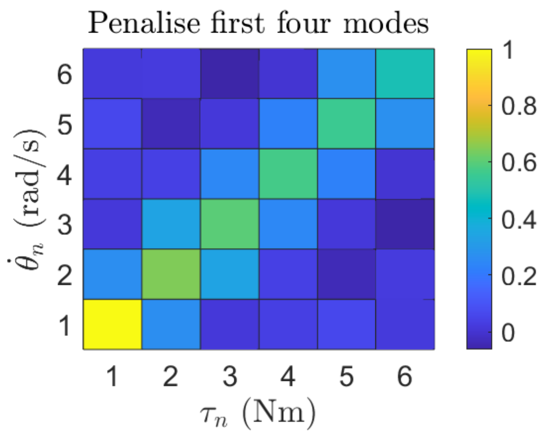

Fig. 4: The LQR feedback matrix when the first four modes are damped. The highest gains are on the diagonal and first upper and lower diagonal, which indicates that the control torque in each joint ideally is a function of its own velocity and that of its first neighbours. The centralised solution can instead by implemented by 6 distributed controllers.

TABLE I: Input energies for the impulse response show that distributed controllers are more efficient than decentralised controllers.

	All modes	First four modes
$\sum u_n^2$	167 (mNm)^2	159 (mNm)^2
Max u_n	6.3 mNm	4.6 mNm

C. Comparison

Both the decentralised and distributed control schemes can be compared in a numerical simulation by means of a torque-impulse response on the first unit cell. The control input in both cases is scaled to be roughly equal such that the comparison is fair. This is done according to two metrics:

1) Sum of the control inputs squared
2) Maximum control torque in the system

The time and frequency response can be seen in Fig. 5. In the frequency responses of the closed-loop systems it can be seen that the distributed controller performs better for the first four lower order modes. This is favourable for many active vibration control applications. The fifth and sixth mode are better damped with a decentralised controller. This is in agreement with the matrices presented in Fig. 3 and 4. The control metrics are given in Table I. It can be concluded that the distributed controllers are more efficient. The maximum control torque in the system is reduced by almost 27%. This makes them suitable for smaller and more lightweight actuators with lower actuator forces. Because each controller is also only dependent on three sensors in the system, it remains practical for implementation in large-scale systems. Especially in large-scale metamaterials where centralised controllers are not feasible, it makes sense to opt for distributed controllers. When damping the entire frequency range is desired, on the other hand, it remains valid to use decentralised controllers.

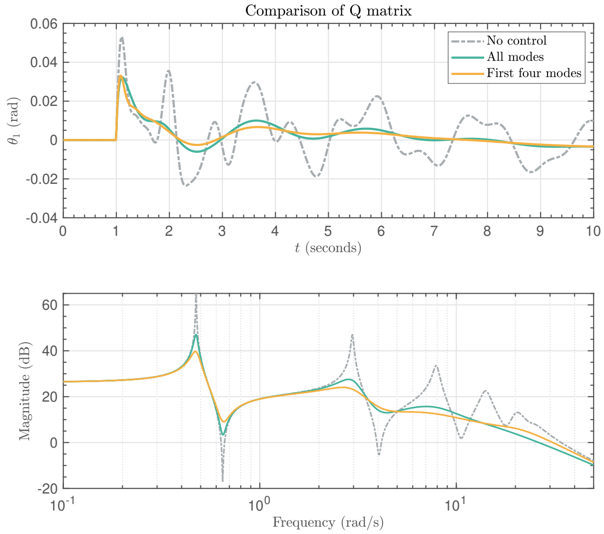

Fig. 5: Time response (top) and frequency response (bottom) of the two closed-loop systems compared to the uncontrolled system.

D. Larger systems

Although the analysis is performed on a system of 6 unit cells, similar numerical results are obtained for larger systems with relative measurements. In Fig. 6, LQR controllers are computed that penalise the first half of the modes fifteen times more than the second half of the modes for $N = 10$ and $N = 20$. The final matrices again show strong localisation around the diagonal and first upper and lower diagonal.

IV. Experimental validation

To verify the numerical simulations, distributed controllers are also experimentally validated for the metamaterial beam of six unit cells.

A. Setup

The metamaterial beam with torque-actuated joints is constructed using rigid 3D printed beams and DC motors as joints. The beam structure is given in Fig. 7. The DC motors (1) can measure the relative angular displacement of the rotor θ_n and

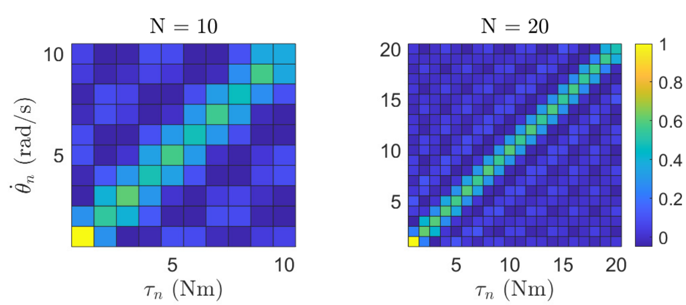

Fig. 6: LQR feedback matrices for two larger systems. In both cases the first $N/2$ modes are damped with q = 15 whereas the second half of the modes is damped with q = 1.

apply a torque τ_n. The unit cells are rigidly connected to each other with blue 3D-printed beams (2). A torsional spring is attached on top of each rotor in the form of a rubber band (3). For small angles, the spring force is only dependent on the relative angular displacement, i.e. $\tau_{\text{spring},n} = k\theta_n$. Each DC motor has a microcontroller installed underneath (4). This can control the unit cell and is also able to send information to its first left and right neighbours through a wired connection. The maximum torque τ_{max} of the motor is 12 mNm, the mass m of each unit cell is 0.2 kg and the torsional spring stiffness k is around 48 mNm/rad. The distance l between unit cells from rotor to rotor is 75 mm.

The communication speed and sampling rate of the system is set to 100 Hz. This is around 20 times higher than the expected maximum frequency content of the system. The measurements of each motor are sent through a digital low-pass filter with cut-off frequency at 5 Hz. The velocity is obtained on the microcontroller by calculating the difference between two sensor measurements in a sample time. Simultaneously, the angular displacement is received from left and right neighbours, which is used to calculate the neighbour velocities.

The robotic structure lies on a horizontal air-table to ensure high vertical stiffness and low friction in traverse directions (5). The beam is clamped on one side to a motion stage (6). This can be moved to the left and right and is used to perturb the system.

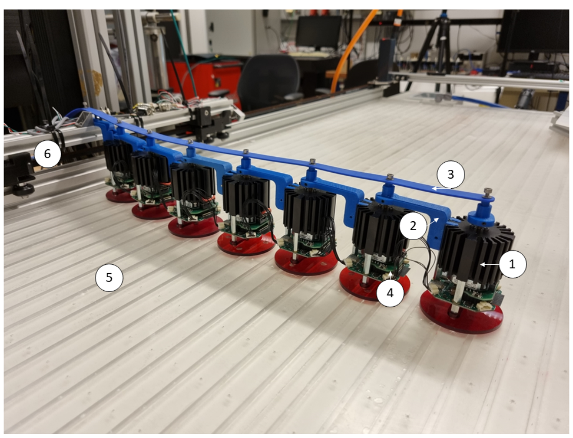

Fig. 7: Experimental setup of the cantilever beam on the air-table. Clamped on one side to a motion stage.

B. Method

Two different perturbations are introduced to validate the numerical simulations: an oscillating perturbation that only excites the second mode of the system and a step input that excites a much larger frequency range. For both scenarios the decentralised controller in Fig. 3 and a truncated version of the distributed controller in Fig. 4 will be used that only includes the diagonal and first upper and lower diagonal gains. The maximum gains are chosen such that the forces are below saturation and similar values for the two relevant control metrics are obtained.

TABLE II: Control metrics for the oscillating perturbation given by the motion stage that excited mainly the second mode.

	Decentralised control	Distributed control
$\sum u_n^2$	7661 (mNm)^2	7560 (mNm)^2
Max u_n	6.2 mNm	5.0 mNm

C. Results

1) Oscillating perturbation: The system is perturbed at a constant frequency at which only the second mode is present. The motion stage is programmed to move at a speed of 50 mm/s, acceleration and deceleration of 1200 mm/s^2 and a back-and-forth displacement of 50 mm, see Fig. 8. The summation of all angular rotations is recorded and given in Fig. 9. The control inputs are given in Table II.

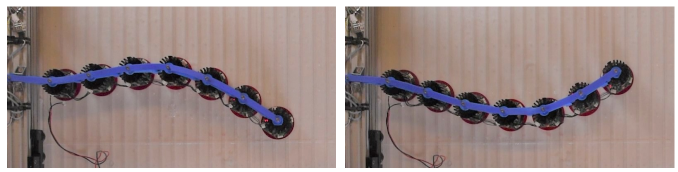

Fig. 8: The motion stage is programmed to mainly excite the second mode demonstrated by the two extremums.

The distributed controllers perform much better than the decentralised ones as the overall amplification is lower. This demonstrates that distributed controllers perform better for the lower order modes of the system. Besides that, the controllers are more efficient. The maximum control torque in the system is 20% lower than with decentralised controllers.

2) Step response: A step response is carried out by moving the motion stage 100 mm with a speed of 500 mm/s and an acceleration and deceleration of 5000 mm/s^2, see Fig. 10. The aim of this perturbation is to excite as many modes and frequencies as possible. The angular deviation of the last unit cell and additionally the summation of all angular displacements can be seen in Fig. 11. The control inputs of the experiment are shown in Table III.

The difference between decentralised and distributed controllers is significantly smaller in this case. As higher frequencies are excited in this test, the benefits of distributed control start to diminish. Still, the highest contributing modes are the low-order modes and the step response has slightly lower peaks with the distributed controller, which conforms the time simulation in Fig. 5.

TABLE III: Control metrics for the step response experiment.

	Decentralised control	Distributed control
$\sum u_n^2$	212 (mNm)^2	224 (mNm)^2
Max u_n	8.9 mNm	6.8 mNm

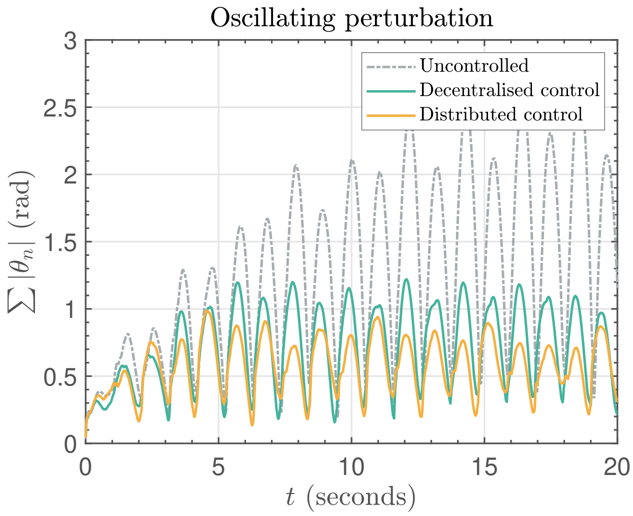

Fig. 9: Absolute output of all unit cells due to an oscillating perturbation.

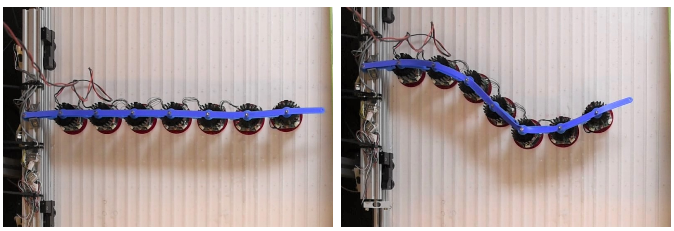

Fig. 10: Visualisation of the beam in rest and after being perturbed.

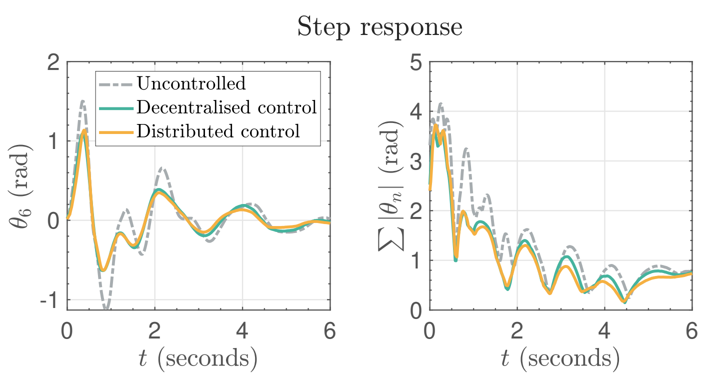

Fig. 11: Step response of the last unit cell and summation of all unit cells. Distributed controllers have slightly lower magnitudes.

V. Conclusion

In this paper we studied the suitability of different control architectures for metamaterials with active damping elements. This was done with the use of LQR in modal domain. It has been shown that effectively damping individual modes requires a fully centralised architecture. However, once multiple modes are penalised some control localisation appears. It has been shown that by damping the whole frequency range, the optimal LQR feedback matrix is reduced to a decentralised solution. Furthermore, we showed that a distributed control architecture is more advantageous for the lower order modes. Compared to decentralised controllers it had superior damping performance, while it remains scalable for implementation in large systems. Besides that, the maximum actuator force is significantly lower, up to 27% in simulation and 20% in experiments compared to a decentralised solution. This is an important result for applications that are limited by actuator force, for example, when using small and lightweight actuators. The obtained results show that centralised solutions like modal control are not needed when only lower order modes need to be damped. This leads to a significant simplification of the control network for systems with many sensors and actuators.

Acknowledgements

We would like to thank Andres Hunt for his help in shaping this publication and for his valuable feedback. Furthermore, we would like to thank Ronald Kortekaas and Kasper van Nieuwland for their assistance on the experimental setup.

References

[1] Y. Liu and X. Zhang, “Metamaterials: A new frontier of science and technology,” *Chemical Society Reviews*, vol. 40, pp. 2494–2507, 4 2011.
[2] R. S. Kshetrimayum, “A brief intro to metamaterials,” *IEEE Potentials*, vol. 23, pp. 44–46, 12 2004.
[3] T. A. Hewage, K. L. Alderson, A. Alderson, and F. Scarpa, “Double-negative mechanical metamaterials displaying simultaneous negative stiffness and negative poisson’s ratio properties,” *Advanced Materials*, vol. 28, pp. 10 323–10 332, 12 2016.
[4] S. Dalela, P. S. Balaji, and D. P. Jena, “A review on application of mechanical metamaterials for vibration control,” *Mechanics of Advanced Materials and Structures*, pp. 1–26, 2 2021.
[5] B. Haghpanah, H. Ebrahimi, D. Mousanezhad, J. Hopkins, and A. Vaziri, “Programmable elastic metamaterials,” *Advanced Engineering Materials*, vol. 18, pp. 643–649, 4 2016.
[6] M. Brandenbourger, C. Scheibner, J. Veenstra, V. Vitelli, and C. Coulais, “Active impact and locomotion in robotic matter with nonlinear work cycles,” 8 2021. [Online]. Available: http://arxiv.org/abs/2108.08837
[7] M. A. McEvoy and N. Correll, “Materials that couple sensing, actuation, computation, and communication,” *Materials science*, vol. 347, 3 2015.
[8] Y. Song, P. C. Dohm, B. Haghpanah, A. Vaziri, and J. B. Hopkins, “An active microarchitectured material that utilizes piezo actuators to achieve programmable properties,” *Advanced Engineering Materials*, vol. 18, pp. 1113–1117, 7 2016.
[9] G. Wang, J. Cheng, J. Chen, and Y. He, “Multi-resonant piezoelectric shunting induced by digital controllers for subwavelength elastic wave attenuation in smart metamaterial,” *Smart Materials and Structures*, vol. 26, 2 2017.
[10] F. Li, C. Zhang, and C. Liu, “Active tuning of vibration and wave propagation in elastic beams with periodically placed piezoelectric actuator/sensor pairs,” *Journal of Sound and Vibration*, vol. 393, pp. 14–29, 4 2017.
[11] K. K. Bera and A. Banerjee, “Ultra-wide bandgap in active metamaterial from feedback control,” *JVC/Journal of Vibration and Control*, 2021.
[12] R. D’Andrea and G. E. Dullerud, “Distributed control design for spatially interconnected systems,” *IEEE Transactions on Automatic Control*, vol. 48, pp. 1478–1495, 9 2003.
[13] M. R. Jovanović and N. K. Dhingra, “Controller architectures: Tradeoffs between performance and structure,” vol. 30. European Control Association, 7 2016, pp. 76–91.
[14] B. Bamieh, F. Paganini, and M. A. Dahleh, “Distributed control of spatially invariant systems,” *IEEE Transactions on Automatic Control*, vol. 47, pp. 1091–1107, 7 2002.
[15] B. Friedland, *Control System Design: An Introduction to State-Space Methods*, ser. Dover Books on Electrical Engineering. Dover Publications, 2012. [Online]. Available: https://books.google.nl/books?id=9WRKZlaCnF8C